

Anatomy of a Bond Cleavage. The Dynamics of Rearrangement of a Strained-Ring Hydrocarbon

Barry K. Carpenter

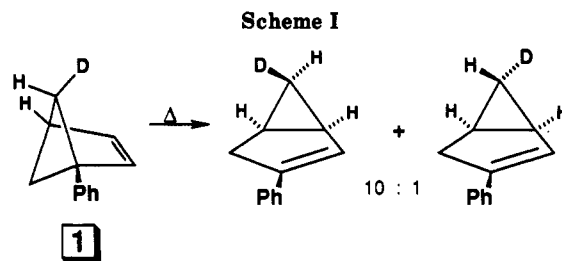
Department of Chemistry, Baker Laboratory, Cornell University, Ithaca, New York 14853-1301

Received March 9, 1992

A theoretical analysis of the formal [1,3] sigmatropic rearrangement of 1-phenylbicyclo[2.1.1]hexene-*endo*-5-*d*, using the AM1-CI model to provide projections of the potential energy surface and extension of a recently developed vector resolution method to evaluate the reaction dynamics, suggests that the preference for inversion of configuration at the migrating carbon observed experimentally in this reaction has nothing to do with conservation of orbital symmetry but is, instead, a result of the detailed dynamics of bond cleavage in the reactant. The results could have application to bond cleavage processes in many strained rings.

Work from this laboratory has shown that the formal [1,3] sigmatropic shift of 1-phenylbicyclo[2.1.1]hexene-5-*d* (1, Scheme I) occurs with a preference for inversion of configuration at the labeled carbon,¹ as predicted by the Woodward-Hoffmann rules,² and in agreement with earlier results on methyl-substituted analogues.³ The preference for inversion is not complete, however, and the product ratio shows no detectable temperature dependence. (The ratio is $(9.99 \pm 0.26):1$ inversion-retention between temperatures of 80.0 and 165.7 °C). This observation renders improbable any explanations for the stereochemistry (including an explanation based on the Woodward-Hoffmann rules) that rely on the existence of different transition states leading to the stereoisomeric products, since the transition states would then have to have coincidentally equal heats of formation. Such a coincidence is made all the more improbable by the fact that we have now observed similar behavior in four different thermal reactions.^{1b,4}

In order to investigate possible explanations for the stereochemistry of rearrangement of 1, the enthalpy surface for the reaction has been explored in three geometrical coordinates, R , θ , and ϕ (defined in Figure 1), using the AM1 semiempirical molecular orbital method,⁵ with configuration interaction involving two electrons distributed in all singlet configurations between the highest occupied and lowest unoccupied molecular orbitals. Such CI is necessary for the proper description of a singlet biradical,⁶ although it may make such species appear too stable with respect to their ground-state precursors because of the "over correction" for electron correlation effects in a semiempirical scheme that is already parameterized to account for electron correlation with single-determinant wavefunctions.⁵ This potential problem, although possibly responsible for the underestimate of the activation enthalpy for the reaction (the calculated ΔH^\ddagger is 19 kcal/mol, whereas the measured value is 28.85 ± 0.23 kcal/mol), was considered not to be of great significance for the present problem since the region of the enthalpy surface that was of primary interest was one in which the values of R would all imply significant biradical character. All geometrical parameters except the three listed were allowed to relax



to their values of lowest energy during the calculations.

As R was increased (with all other geometrical parameters, including θ and ϕ , being allowed to adopt their lowest-energy values) from its initial value of 1.591 Å, the calculated heat of formation was found to rise, until R reached about 2.0 Å. Between $R = 2.00$ and 2.05 Å ΔH_f° was found to remain approximately constant. At greater values of R the calculated ΔH_f° decreased, although the dependence on R was weak. The results are summarized in the graph in Figure 2.

This behavior might lead one to expect the C1-C5 bond to be broken at about $R = 2.0$ Å, but this is far from the case, as revealed by the large barrier to torsion about the C4-C5 bond at $R = 2.0$ Å. A plausible explanation is that at $R = 2.0$ Å there is still significant residual C1-C5 bonding, but the increase in ΔH_f° caused by reduction of this bonding at increased values of R is just matched by a decrease in ΔH_f° caused by relief of strain in the rest of the molecule. Attempted torsion about C4-C5 at $R = 2.0$ Å also reduces the C1-C5 bonding, but the resulting increase in ΔH_f° is not matched by a decrease due to relief of strain. The alternative possibility that the barrier to torsion could be due to incipient bonding between the migrating carbon (C5) and the migration terminus (C3) was ruled out by the observation that the barrier decreased at $R = 2.2$ Å (Figure 4). One would have expected an increase in the barrier to torsion at larger values of R if C3-C5 bonding had been responsible. At $R = 2.4$ Å the barrier to torsion away from the initial value of ϕ was calculated to be near zero. Minima due to C3-C5 bonding started to appear in the enthalpy surface at this value of R (Figure 5).

In the early stages of the reaction, the barrier to torsion would restrict the motions of the atoms of most molecules to those approximately defined by an increase in R and an increase in the pyramidal angle, θ —the latter being due to rehybridization at C5. Significant rotation about the C4-C5 axis is necessary in order to form a product, but the barrier to torsion would inhibit such motion at this stage. The choice between formation of the inversion or retention product depends on the sense of torsion (clockwise or counterclockwise) about the C4-C5 bond, but this decision must await the disappearance of the torsion

(1) (a) Newman-Evans, R. H.; Carpenter, B. K. *J. Am. Chem. Soc.* 1984, 106, 7994. (b) Newman-Evans, R. H.; Simon, R. J.; Carpenter, B. K. *J. Org. Chem.* 1990, 55, 695.

(2) Woodward, R. B.; Hoffmann, R. *The Conservation of Orbital Symmetry*; Verlag Chemie: Weinheim, 1970.

(3) Roth, W. R.; Friedrich, A. *Tetrahedron Lett.* 1969, 2607.

(4) Lyons, B. A.; Pfeifer, J.; Carpenter, B. K. *J. Am. Chem. Soc.* 1991, 113, 9006.

(5) Dewar, M. J. S.; Zoebisch, E. G.; Healy, E. F.; Stewart, J. J. P. *J. Am. Chem. Soc.* 1985, 107, 3902. Calculations were performed on an IBM 3090 using the vectorized version of the program package AMPAC.

(6) Salem, L.; Towland, C. *Angew. Chem., Int. Ed. Engl.* 1972, 11, 92.

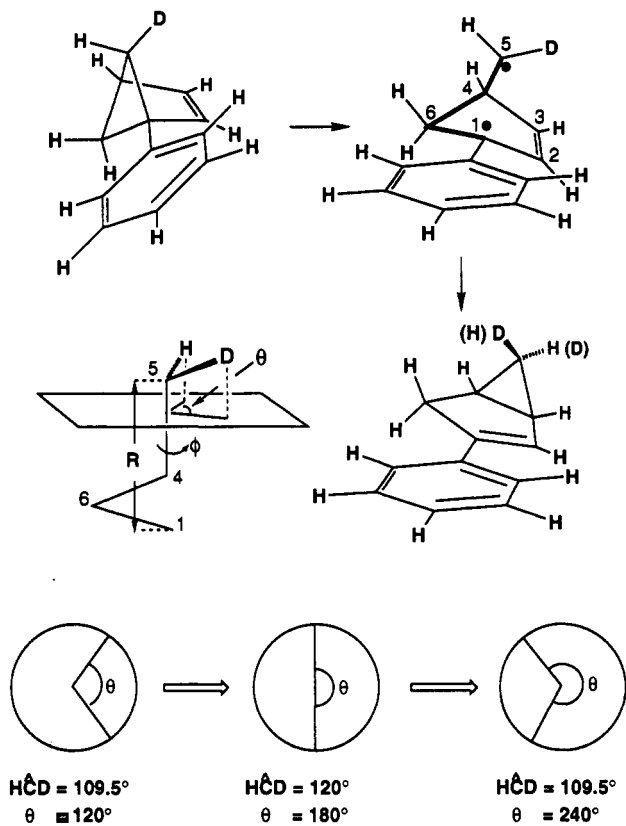


Figure 1. Definition of the three geometrical coordinates, R , θ , and ϕ , used to explore the potential energy surface for rearrangement of compound 1. The angle θ serves to track pyramidal inversion at the labeled carbon, as shown (using idealized HCD angles) in the three circular diagrams at the bottom of the figure. The angle ϕ measures torsion about the C4–C5 bond; it has a value of 0° when the bisector of the HCD angle makes a 0° dihedral angle with the C4–H bond.

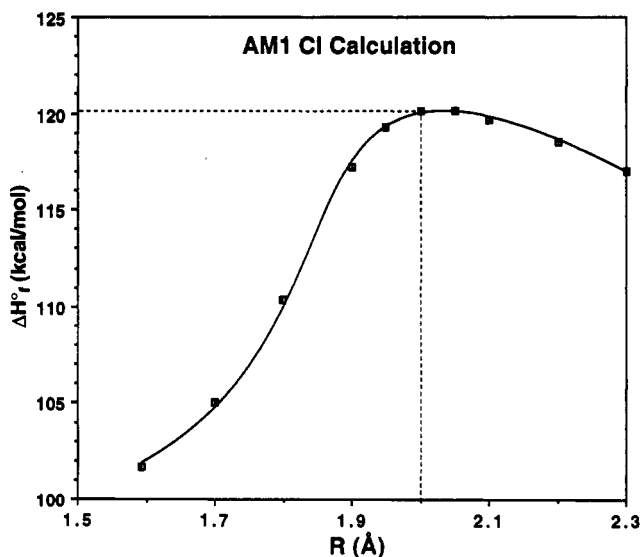


Figure 2. Change in calculated ΔH_f° with increasing R . All other geometrical parameters were allowed to adopt their lowest-energy values.

barrier, which, according to the calculations, does not occur until about $R = 2.4 \text{ \AA}$. Once the barrier has disappeared, the selection of the sense of the torsional motion cannot be made on energetic grounds, but is presumably determined by the efficiency of dynamic coupling of the initial R, θ motion into the two possible senses of ϕ motion. This coupling efficiency can be estimated by an extension of a recently described vector resolution method.⁷

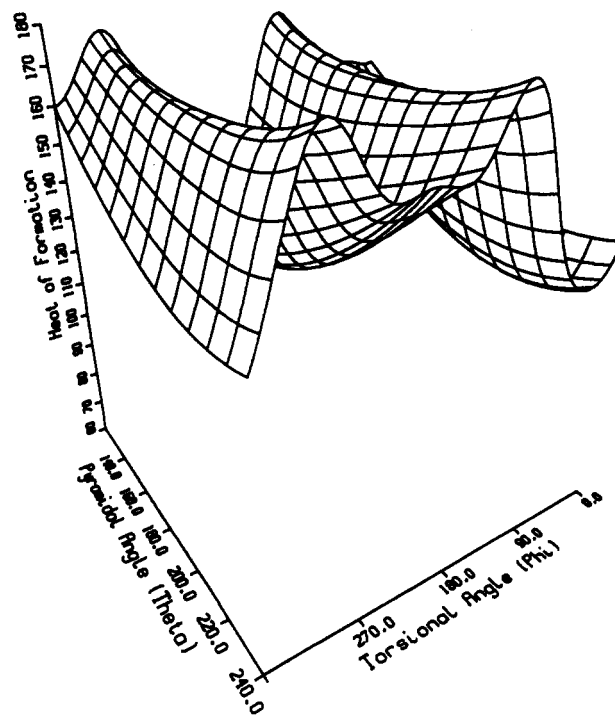


Figure 3. Plot of calculated ΔH_f° vs θ and ϕ at $R = 2.0 \text{ \AA}$. All other geometrical parameters were allowed to adopt their lowest-energy values.

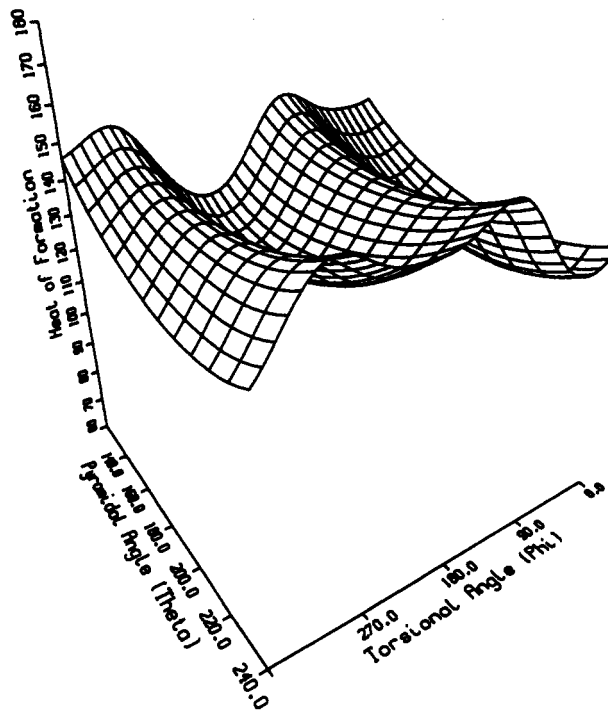


Figure 4. Plot of calculated ΔH_f° vs θ and ϕ at $R = 2.2 \text{ \AA}$. All other geometrical parameters were allowed to adopt their lowest-energy values.

In the original version of the vector resolution method, a dynamically determined product ratio was deduced by comparing components of the reaction-coordinate vector in the directions of the various post-transition-state minima.⁷ The reaction-coordinate vector was determined from a vibrational frequency analysis of the transition state. In the present case, the critical stage of the reaction is calculated to occur at about $R = 2.4 \text{ \AA}$, well beyond the formal

(7) Peterson, T. H.; Carpenter, B. K. *J. Am. Chem. Soc.* 1992, 114, 766.

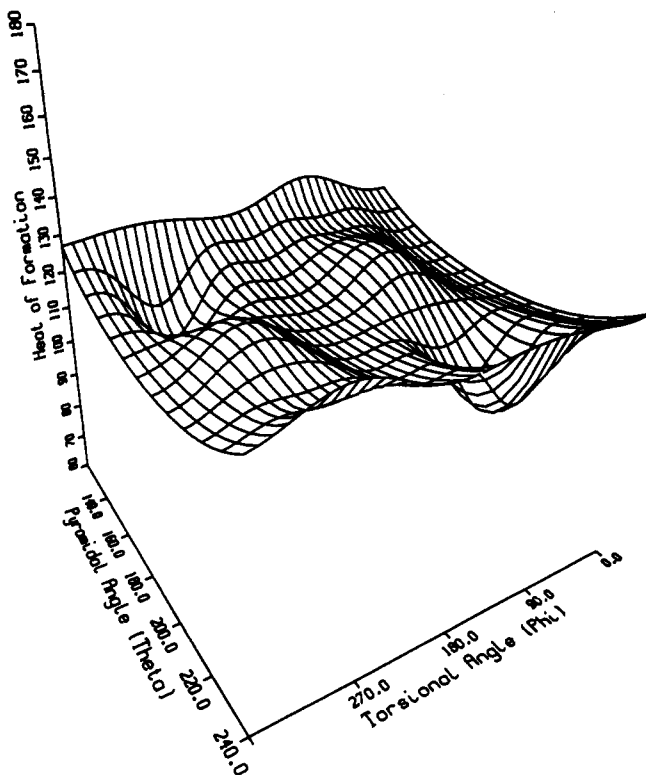


Figure 5. Plot of calculated ΔH_f° vs θ and ϕ at $R = 2.4$ Å. All other geometrical parameters were allowed to adopt their lowest-energy values.

"transition state" for the reaction. In order to evaluate the reaction dynamics, the reaction coordinate vector was thus approximated by computing the vector of mass-weighted atomic displacements (which are primarily R, θ motions, although the motions of all atoms were included) between the minimum energy structure with $R = 2.3$ Å and the critical point at $R = 2.4$ Å where the barrier to torsion is lost. That such a linear-synchronous-transit vector was a reasonable representation of the reaction coordinate in the critical region could be shown by computing the energies of intermediate structures ($R = 2.33$ and 2.37 Å) defined by the vector and showing that their energies fell less than 1 kcal/mol on reoptimization of their geometries at the specified value of R .

The reaction coordinate vector was found to make an angle of 27° with the vector describing a 10° torsion in the inversion direction, but an angle of 152° with the vector describing a 10° torsion in the retention direction.⁸ The smaller angle for the inversion direction implies more efficient coupling of the initial R, θ reaction dynamics into the torsion leading to inversion, in keeping with the experimental observation of the preferential formation of the inversion product. Earlier studies have suggested that such dynamically determined product ratios can show the lack of significant temperature dependence observed experimentally in this case.⁴

In the previously applied example of the vector-resolution model,⁷ it was found that all transformation vectors to the post-transition-state minima made angles of $\leq 90^\circ$ with the reaction-coordinate vector. Under such circumstances the reaction-coordinate vector could be resolved into components perpendicular and parallel to the transformation vectors leading to each energy minimum. The

(8) The internal rotation angles are kept small so that the atomic displacements can be approximated by linear synchronous transit vectors (see ref 5).

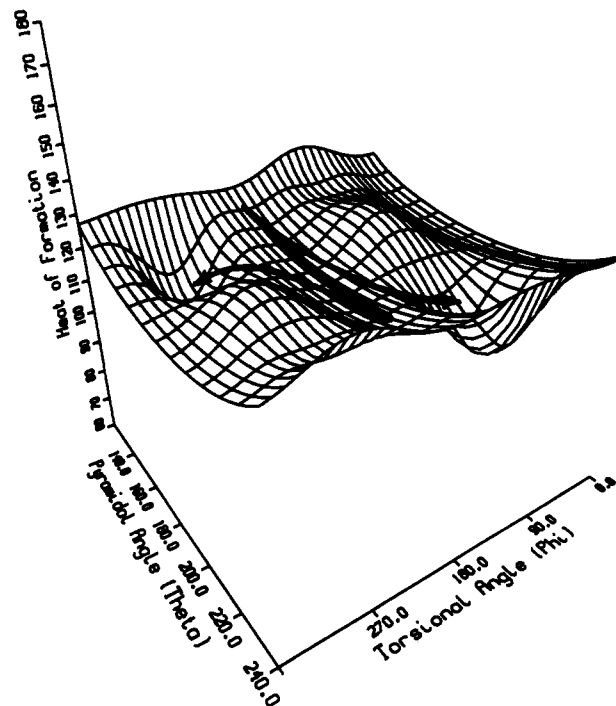


Figure 6. Superimposition of schematic trajectories for formation of inversion and retention products on the plot of ΔH_f° vs θ and ϕ at $R = 2.4$ Å. In reality R is not constant during the reactions implied by the trajectories (see text).

ratio of parallel components was shown to provide a reasonable estimate of the reaction branching ratio.⁷ In the present example the angle between the reaction-coordinate vector and the vector describing torsion in the direction of the retention product is $>90^\circ$. The implication is that the components of the reaction coordinate vector are thus antiparallel and perpendicular to the torsion vector. In physical terms this means that, in order to reach the retention product, the most probable reaction trajectory will involve a reflection of the initial R, θ trajectory, with the product being formed on the transit back to starting material. These more complex dynamics are not amenable to the quantitative analysis carried out previously.⁷ Schematic trajectories for formation of the inversion and retention products are shown superimposed on the θ, ϕ enthalpy surface at $R = 2.4$ Å, in Figure 6. A more realistic representation would show trajectories on the R, θ, ϕ , enthalpy hypersurface, but there is not an easy way to draw such a figure!

The gross features of the potential energy surface calculated for rearrangement of 1-phenylbicyclo[2.1.1]hexene, particularly the persistence of the barrier to torsion after the barrier to C-C stretching has disappeared, are likely to be common in the opening of strained-ring compounds. It therefore seems possible that there might be a similar dynamic preference for inversion of configuration in the opening of many small rings. Such reactions could include those formal [1, n] sigmatropic shifts that are not, in fact, pericyclic reactions (such as the present example).^{9,10}

Acknowledgment. This research was conducted using the Cornell National Supercomputer Facility, a resource Center for Theory and Simulations in Science and Engineering (Cornell Theory Center), which receives major funding from the National Science Foundation and IBM

(9) Carpenter, B. K. *J. Am. Chem. Soc.* 1985, 107, 5730.

(10) It should be noted that the primary evidence in favor of a non-pericyclic mechanism is experimental (the lack of temperature dependence of the product ratio).

Corporation, with additional support from the state of New York and members of the Corporate Research Institute.

Supplementary Material Available: Details of the AM1-CI calculations, consisting of the points used to define the potential

energy surfaces and the functions used to interpolate between the points (5 pages). This material is contained in many libraries on microfiche, immediately follows this article in the microfilm version of the journal, and can be ordered from the ACS; see any current masthead page for ordering information.

Mechanisms and Stereochemistry of Amine Substitution Reactions at the Carbon-Nitrogen Double Bond

James Elver Johnson,* Susan L. Todd, Susan M. Dutson, Abdolkarim Ghafouripour, Reidun M. Alderman, and Martha R. Hotema

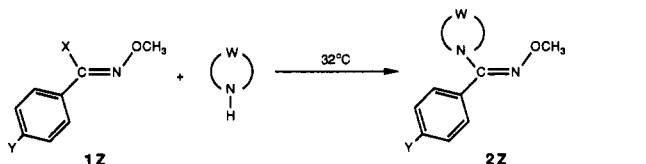
Department of Chemistry, Texas Woman's University, Denton, Texas 76204

Received January 13, 1992

The reaction of (*Z*)-*O*-methyl-*p*-nitrobenzohydroximoyl chloride [4-NO₂C₆H₄C(Cl)=NOCH₃] with morpholine, piperidine, pyrrolidine, and azetidine gives the corresponding (*Z*)-amidoximes [4-NO₂C₆H₄C(NR₁R₂)=NOCH₃]. The rate equations for these reactions in benzene solution contain both first-order and second-order terms in amine. The rates of these reactions increase with increasing basicity [*k*(pyrrolidine) > *k*(morpholine)] and decreasing size of the amine [*k*(azetidine) > *k*(pyrrolidine) > *k*(piperidine)]. The approximate Hammett ρ -values for the reaction of (*Z*)-hydroximoyl chlorides with azetidine are +1.0 for the amine-catalyzed process and 0 for the uncatalyzed pathway. The element effect, *k*(*p*-nitrobenzohydroximoyl bromide)/*k*(*p*-nitrobenzohydroximoyl chloride), is 11.9 for the amine-catalyzed reaction and 8.16 for the uncatalyzed reaction. These results suggest that the reactions proceed by an addition-elimination mechanism (A_N + D_N) in which the amine is deprotonating the zwitterionic tetrahedral intermediate in the amine-catalyzed process. The slow reaction of azetidine in benzene solution with (*E*)-*O*-methyl-*p*-nitrobenzohydroximoyl chloride gives a mixture of the (*Z*)- and (*E*)-amidoxime with the *E* isomer predominating (*E*/*Z* \approx 98:2). The rate equation for this reaction contains first-order and third-order terms in azetidine. It is suggested that the amine-catalyzed route involves nucleophilic attack by an amine monomer to form a tetrahedral intermediate which breaks down with the assistance of an amine dimer (or the homocjugate acid of the amine). The difference in the observed rate equations for (*Z*)- and (*E*)-hydroximoyl chlorides with azetidine is attributed to stereoelectronic effects.

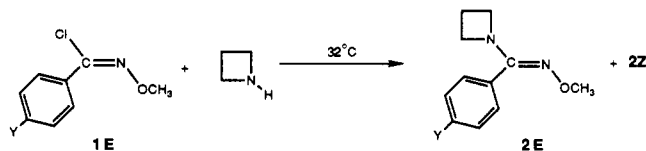
Introduction

The kinetics and stereochemistry of pyrrolidine substitution in (*Z*)-*O*-methylbenzohydroximoyl chlorides (**1Z**) in benzene solution has been reported by us.¹ These



1Za: X = Cl; Y = NO₂
b: X = Y = Cl
c: X = Cl; Y = H
d: X = Cl; Y = CH₃
e: X = Cl; Y = OCH₃
f: X = Br; Y = NO₂
g: X = Br; Y = H

2Za: Y = NO₂; W = (CH₂)₃
b: Y = Cl; W = (CH₂)₃
c: Y = H; W = (CH₂)₃
d: Y = CH₃; W = (CH₂)₃
e: Y = OCH₃; W = (CH₂)₃
f: Y = NO₂; W = (CH₂)₅
g: Y = NO₂; W = (CH₂)₂O(CH₂)₂



1Ea: Y = NO₂
b: Y = Cl
c: Y = H
d: Y = CH₃

2Ea: Y = NO₂
b: Y = Cl
c: Y = H
d: Y = CH₃

substitution reactions gave the (*Z*)-amidoxime **2Z** as the only product. Under pseudo-first-order conditions (excess pyrrolidine) the kinetic equation followed by these reactions contained both first-order and second-order terms in pyrrolidine:

$$k'_{\text{obs}} = k''[\text{amine}] + k'''[\text{amine}]^2 \quad (1)$$

The derived second-order (*k''*) and third-order (*k'''*) rate constants were obtained from plots of the second-order rate constants (*k''*_{obs}) vs pyrrolidine concentration:

$$\frac{k'_{\text{obs}}}{[\text{amine}]} = k''_{\text{obs}} = k'' + k'''[\text{amine}] \quad (2)$$

The third-order rate constants (*k'''*) gave a Hammett ρ -value of +1.06 with σ while the second-order rate constants (*k''*) showed no systematic substituent effect ($\rho \approx 0$). The positive ρ -value on *k'''* and the relatively small element effect (*k''*_{Br}/*k''*_{Cl} = 26.9 and *k'''*_{Br}/*k'''*_{Cl} = 10.1 for **1Za** and **1Zf**) suggested that this reaction proceeds by an addition-elimination mechanism (A_N + D_N, Scheme I). It was suggested that the positive ρ -value for the amine-catalyzed pathway was due to the transition state for *k*₃ (TS-3 in Scheme I) where the second molecule of amine assists the reaction by deprotonating the amino nitrogen. The deprotonation of the amino nitrogen moves some of the positive charge to the second amine molecule, leaving a disproportionate amount of negative charge near the aromatic ring.

Results and Discussion

In an attempt to learn more about the factors that determine the reactivity of amines in nucleophilic substitu-

(1) Johnson, J. E.; Ghafouripour, A.; Arfan, M.; Todd, S. L.; Sitz, D. A. *J. Org. Chem.* 1985, 50, 3348-3355.

(2) Perrin, D. D. *Dissociation Constants of Organic Bases in Aqueous Solution*; Butterworth: London, 1965.

(3) Ta-Shma, R.; Rappoport, Z. *J. Am. Chem. Soc.* 1977, 99, 1845-1858.